Proceedings of
10th European Conference on Turbomachinery Fluid dynamics & Thermodynamics
ETC10, April 15-19, 2013, Lappeenranta, Finland

Circumferential Grooves for a Modern Transonic Compressor: Aerodynamic Effects, Benefits and Limitations

Georgios Goinis, Christian Voß, Marcel Aulich

German Aerospace Center (DLR)
Institute of Propulsion Technology
Linder Höhe, 51147 Cologne, Germany

ABSTRACT

It has been shown in many cases that a notable aerodynamic stability enhancement can be achieved using circumferential grooves on transonic compressors. This advantage, however, often involves degradation in efficiency at design point conditions. In order to analyze the correlations between efficiency, surge margin and other flow quantities on the one hand and the geometric parameters related to circumferential grooves on the other, an automated multi objective geometry optimization of circumferential grooves for a transonic compressor has been performed. For the surge point determination an iterative approach was used to change the static back pressure until the numerical surge limit was determined with a sufficiently small uncertainty.

As a result of the optimization two different types of grooves have been identified. The first type is comparatively small and located only little downstream the leading edge of the rotor. It is capable of increasing the surge margin, while only slightly decreasing efficiency. The second groove type is located more towards the trailing edge and significantly bigger in cross sectional size. It can improve the efficiency of the rotor, but at the same time blockage is generated. Combining the two groove types, also the effects combine, resulting in an increased surge margin and increased efficiency. Applying more than one groove of type one further increases the surge margin compared to a single groove, however the gain is limited. Important groove parameters of optimized grooves are further studied, regarding their sensitivity. The working principles and flow phenomena of the grooves increasing the surge margin are analyzed in detail.

NOMENCLATURE

ADP	Aerodynamic design point	$\dot{m}$	Mass flow rate [kg/s]
CG	Casing groove	m/M	Relative mass flow [-] (0 at hub, 1 at tip)
CFD	Computational fluid dynamics	n	Rotational speed $\left[\frac{1}{min}\right]$
CT	Casing treatment	n_{norm}	Normalized rot. speed $n_{norm} = n/N$ [-]
LE	Leading edge	N	100% rotational speed; $N = 12960 \cdot \frac{1}{min}$
MVDR	Meridional velocity density ratio	w	Groove width [m]
OP	Operating point	x	Groove position [m]
PID	Proportional-integral-derivative	α	Groove upstream angle [°]
RANS	Reynolds-averaged Navier-Stokes	β	Groove downstream angle [°]
RPM	Revolutions per minute	γ	Groove angle of lid [rad]
SM	Surge margin (criterion)	$\eta_{is.OPx}$	Isentropic efficiency at OP x [-]
c_{ax}	Axial chord length [m]	$\eta_{is.WL}$	Efficiency criterion
f	Fitness function	Π_{tot}	Total pressure ratio [-]
h	Groove height [m]	$\Pi_{tot.OPx}$	Total pressure ratio over rotor 1 at OP x

INTRODUCTION

Casing treatments (CTs) are applied to increase the surge margin of a compressor. As CTs influence the flow through the compressor at all operating points, the performance characteristics are also affected at working line conditions, clearly away from the surge margin. This influence of CTs on the flow at design point conditions can be negative, especially regarding efficiency. Therefore the main goal when designing CTs is to increase the surge margin by a maximum and reduce efficiency at the design point by a minimum or, if possible, even increase efficiency.

CTs are usually classified regarding their geometrical shape (see e.g. Hathaway (2007) [7]). One common type are axis-symmetric circumferential grooves (also "casing grooves" or CGs), which are cut into the endwall. So far the design of the grooves is mainly based on empirical results rather than established design criteria. Usually the shape, count and location of the grooves are changed for a limited number of configurations which are then compared to study the flow effects. Only recently specific geometric parameters are analysed extensively, mainly due to the advance in CFD technology. Many of these studies were done for subsonic compressors and only few are available for transonic compressors. But as the flow physics of subsonic and transonic compressors differ significantly the transferability of the results is limited. Furthermore, the results are sometimes contradictory regarding an optimal design of the groove, underlining the need for further research.

Recent studies of CGs for transonic compressors, comparing different groove geometries and configurations, have been done, amongst others, by Rabe und Hah (2002) [12], Perrot et al. (2007) [11] and Müller et al. (2007) [10]. Rabe und Hah (2002) [12] conclude from their numerical and experimental studies that the traditional assumption that shallow grooves are inferior to deeper grooves does not hold for transonic compressors and better results can be obtained with shallow grooves. Furthermore they found that two shallow grooves near the leading edge are more effective than five grooves from leading to trailing edge and concluded that grooves placed near the leading edge are more efficient. They assume that the main mechanism leading to the increase in surge margin of the grooves is an alteration of the local flow distribution near the pressure side of the leading edge, which can be measured by how much the flow incidence at the pressure side of the leading edge is reduced.

Perrot et al. (2007) [11] conducted a numerical investigation and found that only grooves close to the leading edge of the rotor are improving the results, as grooves more to the trailing edge of the rotor do not overlay the tip leakage vortex trajectory. They assume that CGs improve the surge margin by delaying the shift of the entropy frontier between the main flow and the secondary tip leakage flow to the inlet. The overall performance is increased by weakening the disturbing eddy zone.

Müller et al. (2007) [10] studied experimentally and numerically different shallow and deep groove configurations and found the deep grooves to be more effective in increasing the operating range. Furthermore they found a higher coverage of the projected axial chord to be favourable in delaying stall inception towards lower mass flow rates. The deep grooves they examined could maintain the efficiency levels compared to the smooth wall configuration and the shallow grooves could even increase efficiency significantly. The grooves were found to reduce the blockage area inside the passage at small mass flow rates. They also found that the tip leakage flow gets deflected towards the axial direction much earlier.

An experimental and numerical parametric study varying the axial location of a single casing groove on a subsonic compressor has been done by Houghton & Day (2011) [8]. Two good groove locations for improving the surge margin are identified. One close to the leading edge and the second at about 50% chord. Shallow grooves offer higher efficiency with only slightly lower surge margin improvement.

Numerical and experimental studies with different groove numbers and sizes have been conducted byWu et al. (2010) [17]. They analyzed the impact of different groove parameters, such as width and height, on the surge margin extension capabilities of the grooves and studied the flow effects.

Automated optimization procedures are now very popular in the aerodynamic design of compressors. First optimization studies related to CGs have been conducted by Choi et al. (2010) [4] and Carnie et al. (2011) [3]. Choi et al. (2010) [4] showed an optimization of circumferential grooves for NASA Rotor 37, with two free parameters, groove width and depth. Carnie et al. (2011) [3] optimized casing grooves for NASA Rotor 37 using a zipper layer meshing method. They allowed six grooves to change in height independently. The width of the grooves also could change and was the same for all grooves.

In this paper the groove design parameters are studied based on the results of an automated optimization. The analysis of the optimization data base helps to uncover and understand correlations between the geometrical parameters and the performance values of optimized grooves. Studying the results of a single groove optimization avoids mixing the effects of different grooves. Important parameters found are further analyzed. Groove combinations are studied and an aerodynamic analysis of the grooves is performed.

TEST CASE

The test case used for this study is the first stage of DLR‘s research compressor Rig250 (see figure 1 and for further details Johann et al. (2008) [9], a 4.5 stage transonic axial compressor. The computational domain includes the IGV as well as the first rotor and stator. The main design parameters of Rig250 are listed in table 1.

RPM (100%)	12960 [1/min]
Reduced mass flow rate	46.3 [kg/s]
Total pressure ratio	4.82 [-]
Ma_{rel} (rotor 1 inlet, ADP)	1.21 [-]

Table 1: **Specifications of Rig250**

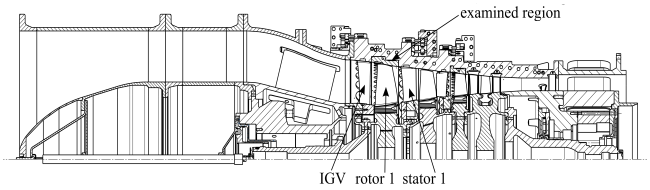

Figure 1: **Rig250 flow path**

To effectively increase the surge margin by applying CTs the rotor has to be tip critical, i.e. surge must originate near the end wall (Greitzer et al. (1979) [6]). Only then can the CTs affect the flow close to the location where the instability evolves. The onset of (numerical) surge of the test configuration has been analyzed for different speed lines to be sure the configuration used in this study is tip critical. To avoid any possible doubt as to where the instability arises, the stator is closed by 8° for $n_{norm} = 90\%$.

The grid used for the optimization is block-struktured and consists of approximately 1 million cells, with a radial resolution of 35 cells and a tip clearance resolution of 7 cells. For validation purposes a grid with 77 cells in radial direction and approximately 2 million cells in total was used.

OPTIMIZATION METHOD

In order to optimize CTs, it is necessary to determine the surge margin for every new CT geometry during the optimization. The more accurate the surge margin shall be determined, the more computational effort is needed. This can be a crucial aspect for a complex optimization using costly CFD. Therefore, a determination of the surge margin with a high accuracy is so far only used in studies comparing a very limited number of cases.

For extensive optimizations, simulating hundreds of different geometries, the evaluation of the surge margin is often based on a single operating point close to the stability limit. The assessment of the surge margin is done indirectly by evaluating the flow values at this specific operating point (see e.g. Siller et al. 2009 [15]). Such a strategy has the advantage of needing only one CFD simulation to predict the surge margin but it is more approximate.

To the authors knowledge a procedure to determine the surge margin with a high accuracy, needing numerous CFD simulations has not been applied in an automated optimization so far. Such a procedure is used in the optimization study at hand for the evaluation of the CTs. This yields in a considerably higher computational effort to evaluate the surge margin of new CT designs. However, the low uncertainty in predicting the numerical surge limit of the CTs is seen as a necessity to obtain the desired information on relations between geometric and performance parameters, justifying the additional computational effort needed. On the other hand a sufficient number of geometries that can be simulated with the computational resources available has to be guaranteed for a successful optimization. Therefore the computing time needed for the evaluation of one CT design (one process chain run) during the optimization should not exceed certain limits. Setting up the optimization one has to weigh up solution accuracy against total number of members that can be obtained using the same amount of computational resources. It this context it is important to notice that the demands on the CFD setup are different for optimizations compared to non-optimization cases. For an optimization it is sufficient to obtain qualitatively correct results. It is not necessary to get the absolute values right. Regarding, e.g., the surge margin, the study at hand is based on the assumption that geometries reaching a higher numerical surge margin during the optimization will also reach a higher surge margin in reality; but the absolute values might be different.

A brief overview of the optimization setup is presented in the following. A more detailed description can be found in Goinis et al. (2012) [5].

Optimization tool and CFD solver

The optimization has been carried out using the DLR Institute of Propulsion Technology's optimization tool *AutoOpti*. *AutoOpti* is based on an evolutionary algorithm with surrogate modelling. Kriging and neural networks are used as surrogate models. *AutoOpti* has the capability of optimizing two or more fitness functions simultaneously ("multi-objective optimization"). *AutoOpti* allows specifying arbitrary process chains which will be sequentially processed for each member during the optimization. Further information on *AutoOpti* can be found in Voß and Siller (2009) [15].

The CFD solver used in conjunction with the optimization tool is the Navier-Stokes solver *TRACE*, which is being developed specifically for turbomachinery flows at the DLR Institute of Propulsion Technology. Details on *TRACE* can be found in Ashcroft et al. (2010) [1] and Becker et al. (2010) [2]. A comparison of numerical results of CT flows obtained using *TRACE* and experimental data, showing good agreement, can be found in Voges et al. (2011) [16] and Schnell et al. (2011) [14].

Groove Parameterization

The grooves are defined by six parameters, as shown in figure 2. The value ranges used for the optimization are listed in table 2. Groove width, height and axial position are normalized using the axial chord length at rotor tip c_{ax}.

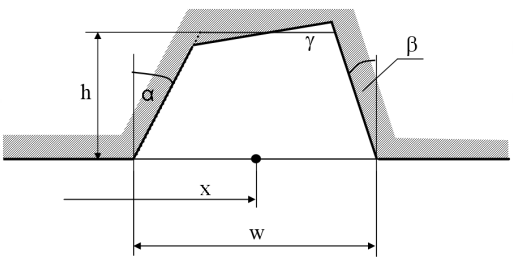

Figure 2: **Groove parameterization**

Parameter	Symbol	Min	Max
Groove position	x	$-0.3 \cdot c_{ax}$	$1.3 \cdot c_{ax}$
Groove width	w	$0 \cdot c_{ax}$	$0.3 \cdot c_{ax}$
Groove height	h	$0 \cdot c_{ax}$	$0.3 \cdot c_{ax}$
Upstream angle	α	$-75°$	$75°$
Downstream angle	β	$-75°$	$75°$
Angle of lid	γ	$-34°$	$34°$

Table 2: **Free groove prarameters**

Surge Point Determination

The surge margin is determined using an iterative approach ("bisection method"), which adapts the back pressure of the compressor in several simulation rounds until a further increase of back pressure by $\Delta p_{min.step} = 10Pa$ would lead to a failure in convergence, based on the defined convergence criteria. In this way the numerical surge point is defined.

Process Chain

The process chain used by to evaluate new grooves consists of the following main steps:

1. Parameter based generation of the groove geometry.
2. Automated meshing
3. RANS CFD simulation of operating point 1, working line, $n_{norm} = 100\%$ (ADP).
4. RANS CFD simulation of operating point 2, working line, $n_{norm} = 90\%$.
5. RANS CFD simulation of operating point 3, near surge, $n_{norm} = 90\%$, adjusted using the automated surge point detection as described above.
6. Calculation of fitness function values.

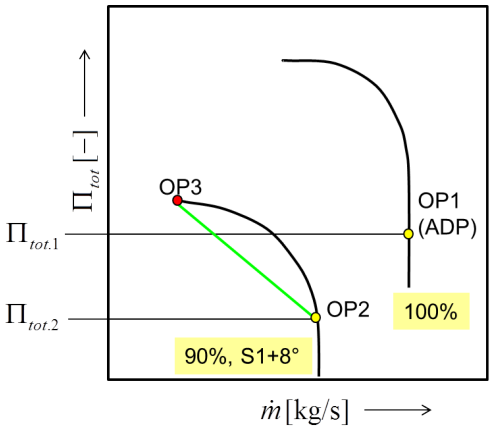

Figure 3: Operating points

The operating points are depicted schematically in figure 3. OP1 and OP2 are adjusted to constant total pressures using a PID controller that works in-line with the CFD code. OP3 is adjusted using the automated surge point determination technique as described above. The convergence criteria for the CFD simulations are the same for all members of the optimization. They are based on efficiency, mass flow and density residuum. At $n_{norm} = 100\%$ the stator is at reference position, whereas at $n_{norm} = 90\%$ it is closed by $8°$, as already mentioned.

Two fitness functions are used during the optimization aiming at increasing the surge margin and efficiency:

1. Efficiency criterion; defined as a weighted sum of the working line efficiencies at $n_{norm} = 90\%$ and $n_{norm} = 100\%$ calculated between IGV entry and stator 1 exit:

$$\eta_{is.WL} = \frac{2 \cdot \eta_{is.OP1} + \eta_{is.OP2}}{3} \tag{1}$$

2. Surge margin criterion, as a comparison of surge to a reference value, as introduced by Reid and Moore (1978) [13]; defined between operating points 2 and 3:

$$SM = \frac{\Pi_{OP3}}{\Pi_{OP2}} \cdot \frac{\dot{m}_{OP2}}{\dot{m}_{OP3}} - 1 \tag{2}$$

OPTIMIZATION RESULTS

The fitness function values of the optimization data base are plotted in figure 4. A remarkable feature is the kink of the Pareto front at the position where the smooth wall geometry lies. Taking into account the position of the grooves x_{rel} it becomes clear that the Pareto front in fact is the result of two overlapping Pareto fronts which intersect exactly at the point in the fitness function space, where the smooth wall geometry lies. This suggests that two sub-areas of the design space have been identified and optimized and the main parameter that defines the belonging of a member to one of the two design spaces is the axial position of the groove x_{rel}.

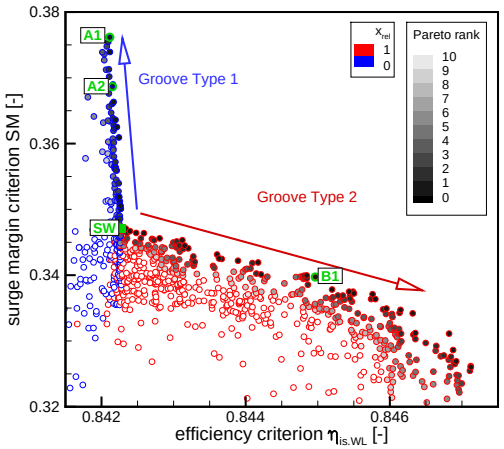

Figure 4: **Optimization data base (shown are Members with Pareto rank > 10)**

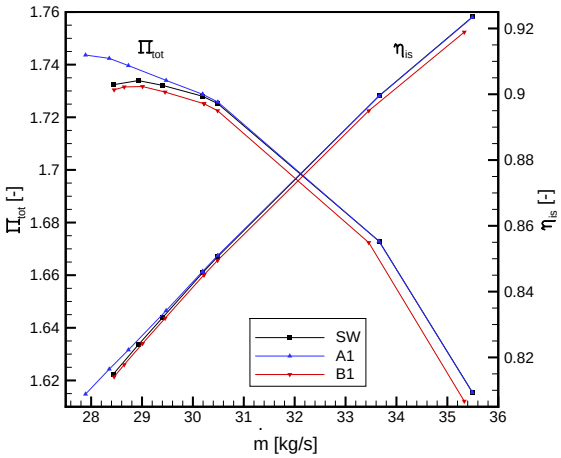

Figure 5: **Speed lines of A1, B1 and smooth wall configurations,** $n_{norm} = 90\%$

Parameter	Groove Type A	Groove Type B
Surge Margin	improves	reduces
Efficiency at ADP	slightly reduces	improves
Position	Close to rotor LE $x_{ax} \approx 0,1 \cdot c_{ax}$	In the rear part of blade $x_{ax} \approx 0,85 \cdot c_{ax}$
Shape	upstream bend shape, low angle at the downstream edge of the groove	quadratic shape
Cross sectional area	comparatively low, slightly increasing for higher surge margins	comparatively high, strongly increasing for higher efficiencies

Table 3: **Groove Type Characteristics**

It can be concluded that effectively two independent optimizations of two different groove types have been conducted at the same time. One Pareto front represents grooves in the front section ($x_{rel} < 0.5$), the other in the aft section ($x_{rel} > 0.5$). The grooves in the front section, in the following denoted as type A grooves, increase the surge margin and slightly decrease efficiency. The grooves in the rear section, in the following denoted as type B grooves, increase efficiency but decrease the surge margin.

Analyzing the groove parameters along the Pareto front, the main design characteristics of the two groove types can be concluded. Important groove parameters are position x_{rel}, size (mainly the width w) and shape for groove type A. A more detailed analysis of the parameters can be found in Goinis et al. (2012) [5]. The general characteristics of the two groove types are summarized in table 3. Typical grooves of each type are shown in figures 6-8. The fitness function values of these members, denoted as A1, A2 (type A) and B1 (type B), are highlighted in figure 4.

The $n_{norm} = 90\%$ speed lines of two grooves and the datum design are plotted in figure 5. The impact of groove A1 on the speed line can be observed for low mass flows only. Total pressure ratio and efficiency of the rotor increase and the surge margin is extended. For higher mass flows the difference between groove A1 and the smooth wall configuration is negligible. The speed line of groove B1 on the other hand is clearly offset compared to the smooth wall configuration towards a

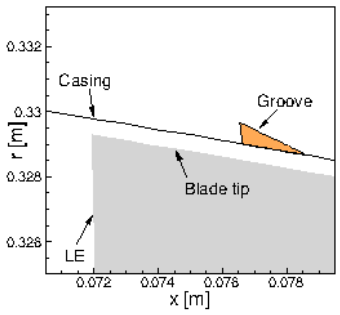

Figure 6: **Groove A1**

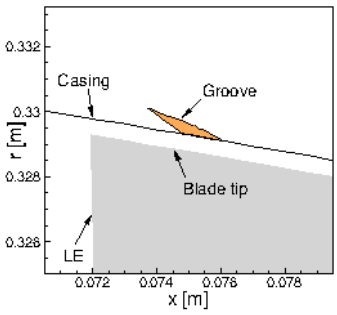

Figure 7: **Groove A2**

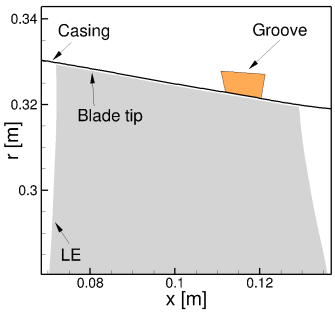

Figure 8: **Groove B1**

lower pressure ratio and lower efficiency. The impact on the surge margin is negative but small.

The effect of the grooves at ADP ($OP1, n_{norm} = 100\%$) and on the fitness function values is listed in table 4. Groove A1 has an increased surge margin with nearly no impact on the ADP values. Groove B1 has a slightly lower surge margin but a higher value of the efficiency criterion $\eta_{is.WL}$, due to a higher efficiency at OP1 $\eta_{is.OP1}$.

In order to check the influence of the groove mesh on the results, groove A1 has been approximated by a slightly different geometry (A1x) allowing to produce a different mesh (see figure 9). The $n_{norm} = 90\%$ speed lines and surge margin of these two grooves are practically identical.

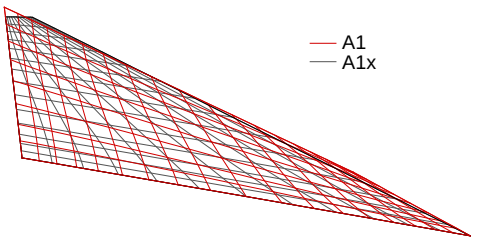

Figure 9: Mesh of groove A1 and A1x

Groove type B has a positive effect on the efficiency at the ADP. To increase efficiency CTs are expected to reduce the losses generated by secondary flows. However, the blockage at rotor exit is higher with the groove compared to the smooth wall configuration. What can be observed in this case is an artificial contraction of the flow path evoked by an additional blockage due to the groove. This results in a redistribution of the mass flow and blade loading towards lower blade sections, what is beneficial in terms of efficiency for the rotor examined. However, the redistribution has a significant effect on the rotor outflow. It can be expected that the following stages will not have an optimal inflow anymore. Therefore the effect should be considered with caution. Up to a certain degree this mechanism can be beneficial without harming the following stages, but in general it is not how a CT is intended to work. Instead of generating an artificial contraction through blockage by a CT, an improved casing design is expected to provide a similar result, but without the unfavourable generation of blockage. The following analysis mainly focuses on grooves of type A. A more detailed analysis of the effects associated with grooves of type B can be found in Goinis et al. (2012) [5].

GROOVE COMBINATIONS

It is now analyzed how more than one groove is influencing the performance of the compressor. Two questions shall be answered:

1. Is it possible to combine the two groove types and benefit from the positive effects of both types? This would give the opportunity to use a groove of type B to compensate the losses in efficiency a groove of type A generates.

2. Can the effect of groove type A be maximized by applying multiple grooves of type A?

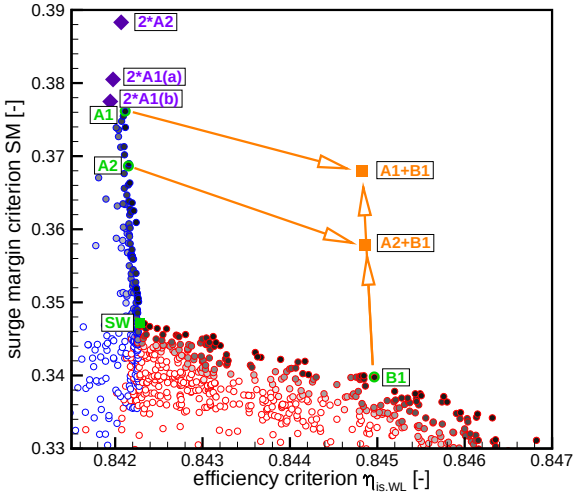

Figure 10: **Groove combinations**

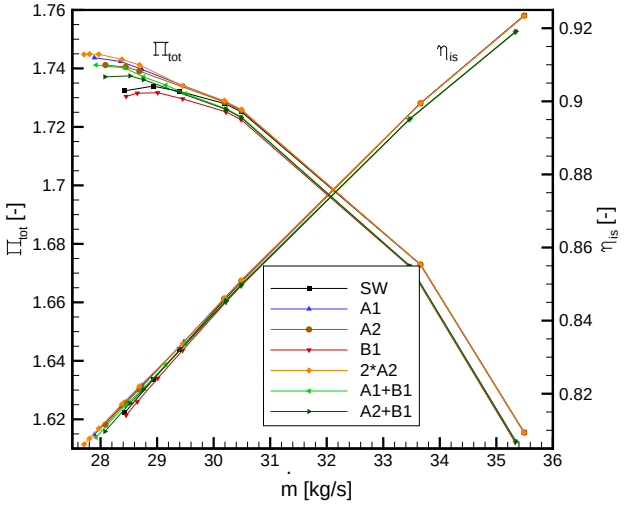

Figure 11: **Speed lines,** $n_{norm} = 90\%$

Member	$\eta_{is.WL}$ [%]	SM [-]	x_{rel} 1st [-]	x_{rel} 2nd [-]	x_{rel} 3rd [-]	$\eta_{is.OP1}$ [%]	$\dot{m}_{OP1}$ [kg/s]	$\dot{m}_{surge}$ [kg/s]
SW	84.22	0.346	-	-	-	85.4	39.60	28.47
A1	84.21	0.376	0.10	-	-	85.3	39.59	27.93
A2	84.22	0.366	0.06	-	-	85.3	39.60	28.13
B1	84.50	0.338	0.10	-	-	85.8	39.58	28.49
2*A1(a)	84.20	0.380	0.10	0.19	-	85.3	39.59	27.83
2*A1(b)	84.19	0.377	0.10	0.15	-	85.3	39.59	27.91
2*A2	84.21	0.388	0.06	0.12	-	85.3	39.60	27.67
3*A1(a)	84.18	0.390	0.03	0.08	0.13	85.3	39.59	27.64
3*A1(b)	84.18	0.388	0.05	0.09	0.13	85.3	39.59	27.66
3*A1(c)	84.19	0.378	0.08	0.13	0.18	85.3	39.59	27.88

Table 4: **Simulation results of different optimized grooves, combinations and the SW**

Combining Grooves of Type A and B

It can be observed that the effects of the grooves can be combined (see figures 10 and 11). Therefore the negative effect on efficiency of a groove type A can be compensated using an additional groove of type B. This proves that the flow mechanisms of the different groove types are independent and can be treated separately. In order not to have a considerable negative effect on the rotor outflow a not too big groove of type B should be used.

Multiple Grooves of Type A

It can be noted that the surge margin can further be extended by applying a second groove of type A. The increase in surge margin for groove A2 (figure 7) can nearly be doubled. However, the benefit in surge margin when applying a second groove A1 is only marginal. Two different positions of the second groove have been tested.

As stated before the optimal position for the groove is at $x_{rel} \approx 0.1 c_{ax}$. Groove A1 is already at this position. Groove A2 is positioned a little more to the leading edge. The second groove of A2, can therefore be placed closer to the optimum of $x_{rel} \approx 0.1 c_{ax}$ compared to the additional grooves of A1

(see table 4 for the axial locations). Using three grooves of type A1 at different positions also shows the influence of the position on the surge margin.

It can be concluded that a compressor with a single groove of type A can further be improved regarding the surge margin using additional grooves. However the benefit depends on the location of the grooves, which have to be close to the optimum location of $x_{rel} \approx 0.1 c_{ax}$. Therefore using two grooves it can be beneficial to position the first groove a little upstream the optimal position of a single groove. Generally the importance of the position of the grooves puts a limitation on the possibility of further improving the surge margin using additional grooves. Using three grooves at different axial locations only marginally increases the surge margin compared to the best value obtained with two grooves (see table 4).

GROOVE PARAMETER SENSITIVITY ANALYSIS

The optimization results show a strong dependency of the groove effectiveness on several groove parameters. The sensitivity of these parameters on the results is analyzed for grooves of type A, which are increasing the surge margin.

Different grooves are varied in axial position from rotor leading edge to trailing edge. The grooves used are A1 and B1 from the optimization and additionally a rectangular groove, denoted as Q1 of roughly the same dimension as groove A1. The resulting fitness function values are plotted in figures 12 and 13. This analysis confirms the result of the optimization. The groove has to be applied at a very distinct position to have a positive effect on the surge margin. This position is at $x_{rel} \approx 0.1 c_{ax}$.

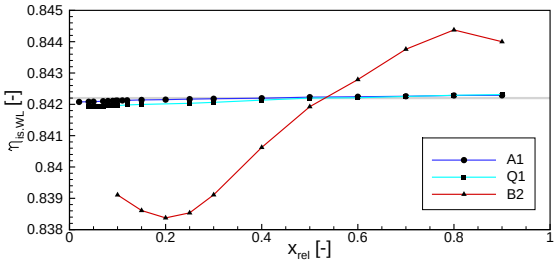

Figure 12: **Efficiency criterion**

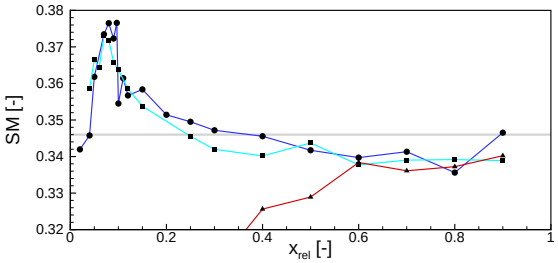

Figure 13: **Surge margin criterion**

Comparing the fitness function values of the grooves A1 and Q1, it can be observed that A1 and Q1 nearly have the same surge margin characteristics. However the efficiencies are lower for Q1. It can be concluded that the shape of the optimized grooves with a low angle at the downstream edge of the groove has evolved during the optimization mainly due to efficiency reasons. The low angle is assumed to be beneficial at conditions clearly away from surge where the groove is not intended to work and no flow should enter the groove. A variation of the downstream angle for groove A1 supports this assumption.

A positive effect on surge margin can only be observed for grooves of a small cross sectional area (type A). Grooves with a bigger cross sectional area (type B) cannot positively influence the surge margin. In order to analyze the importance of the size of the groove, groove A1 is scaled. It is found that for sizes more than two times the original size and less than half of the original size a positive effect on the surge margin cannot be observed anymore.

It can be concluded that certain geometric parameters of the groove are very sensitive regarding the effectiveness of the groove in increasing the surge margin. It cannot be assumed that optimal groove parameters, especially regarding the groove position, are the same for every compressor.

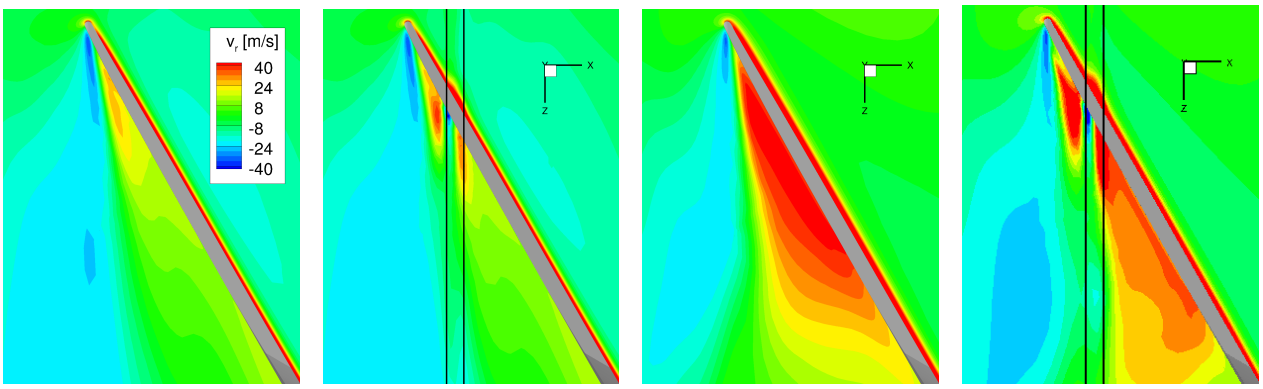

(a) SW OP1 (b) A1 OP1 (c) SW Near Surge (d) A1 Near Surge

Figure 14: **Radial velocities at blade tip; (a) and (b):** $n_{norm} = 100\%$**, OP1; (c) and (d):** $n_{norm} = 90\%$**, near surge.**

AERODYNAMIC ANALYSIS OF GROOVES TYPE A

Groove type A primarily influences the flow close to the surge margin. The location of the groove close to the leading edge of the rotor blade is ideal to influence the evolving tip leakage vortex.

Furthermore the pressure difference between pressure and suction side in the front part of the blade strongly depends on the throttling condition of the rotor and the position of the shock. At operating points close to surge there is a significant pressure difference between pressure and suction side of the blade at the groove position. This results in a flow through the groove from pressure to suction side.

For operating points close to the working line with a passage shock downstream the groove the influence of the groove on the flow is very local only. For such operating points the flow below the groove in the passage is supersonic at all circumferential positions. Due to the lower throttling and the different position of the shock the pressure difference between suction and pressure side of the blade at the position of the groove is significantly lower. As this pressure difference is driving the flow through the tip gap and the groove above the rotor, the mass flow from pressure to suction side is also lower.

In figure 14 the radial velocity of the flow close to the casing is plotted. It can be observed that the flow enters the groove at the pressure side of the blade and leaves it at the suction side. For an operating point at working line conditions the flow velocities are significantly lower and the difference between the grooved casing and smooth casing configuration are small compared to an operating point near surge.

At operating points away from surge even the flow through the groove from pressure to suction side of the blade is very limited. Therefore the effect of the groove at such operating points on the general performance characteristics of the compressor is very low. It only starts to increase close to surge with the shock moving upstream and past the groove at the pressure side of the blade and the pre shock Mach number increasing.

What can be observed in general is the fact that the flow into and out of the groove mainly happens close to the blade. At other circumferential positions, the flow passes the groove without entering it. The low angle at the downstream end of the groove promotes this condition.

A comparison of a configuration with one groove (A1), with two grooves (2*A2) and without a groove at $n_{norm} = 90\%$ close to the stability limit for an identical mass flow of $\dot{m} = 28.5kg/s$ (denoted as ”near surge”) shows how the tip leakage vortex is getting influenced by the groove flow (see figure 15).

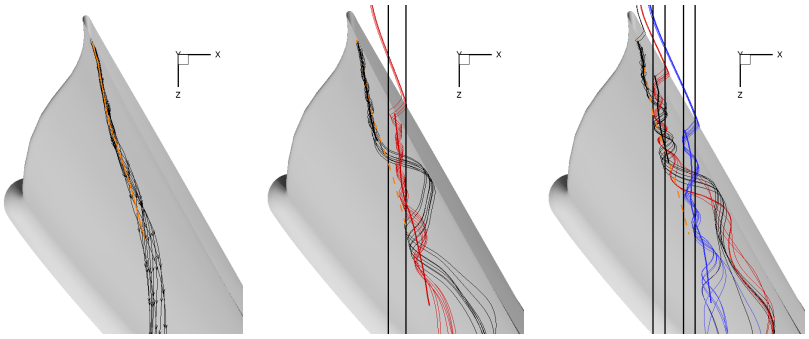

(a) SW (b) A1 (c) 2*A2

Figure 15: **Vortices near surge, $n_{norm} = 90\%$; stream traces of tip leakage vortex and vortices evolving at the grooves. Dashed line in (b) and (c): vortex core of tip leakage vortex of the SW case.**

It can be observed that at each groove an additional vortex develops. As the vortices that evolve all have the same rotational direction and propagate in parallel the flow at their contact point is in opposite direction and hence they cannot coexist and must interact. Considering the case with one groove (A1) the additional vortex interacts with the tip leakage vortex which is being diverted and passes the additional vortex from below. It then starts mixing up with the additional vortex. For the case with two grooves the same mechanism occurs a second time. The tip leakage vortex mixes with the vortex which develops at the first groove and the resulting flow passes below the vortex developing at the second groove.

As a result this vortex interaction has a positive influence on the flow close to surge. The turbulent kinetic energy in the tip area can be reduced (see figure 16). Also the blockage is reduced (see figure 17). The mass flow through the tip gap (and groove) is reduced compared to the smooth wall configuration by approximately 20%, while increased at ADP by approximately 5% only. Comparing the isentropic Mach distributions for an airfoil at 98% blade height at different throttling conditions (see figure 18) it can be observed that the shock position for the grooved configuration close to surge at an identical mass flow rate of $28.5kg/s$ is more downstream, indicating the grooves potential to increase the surge margin. Again at lower throttling rates the difference between grooved and smooth wall configuration is only marginal and can be observed very close to the position of the groove only. The interaction of the tip leakage vortex with the groove flow and the bow shock explains why the position of the groove of type A is so important to obtain the desired result.

CONCLUSION

An automated optimization of a single circumferential groove type casing treatment has been carried out in order to analyze the correlations between geometrical parameters and performance values. Two different types of grooves have been identified by analyzing the geometrical parameters of the optimized grooves in relation to the optimization objectives; an increased surge margin and an increased efficiency at working line conditions. The two groove types differ in their geometrical properties and in the way they influence the flow. The main geometrical difference of the two groove types is their axial position. Other parameters found to be important are the width, size and downstream angle of the groove.

The first groove type is capable of increasing the surge margin, with slight losses in efficiency (type A). The second groove (type B) increases the efficiency at design point conditions, but has a negative effect on the blockage and outflow conditions of the rotor. The effects of the two groove

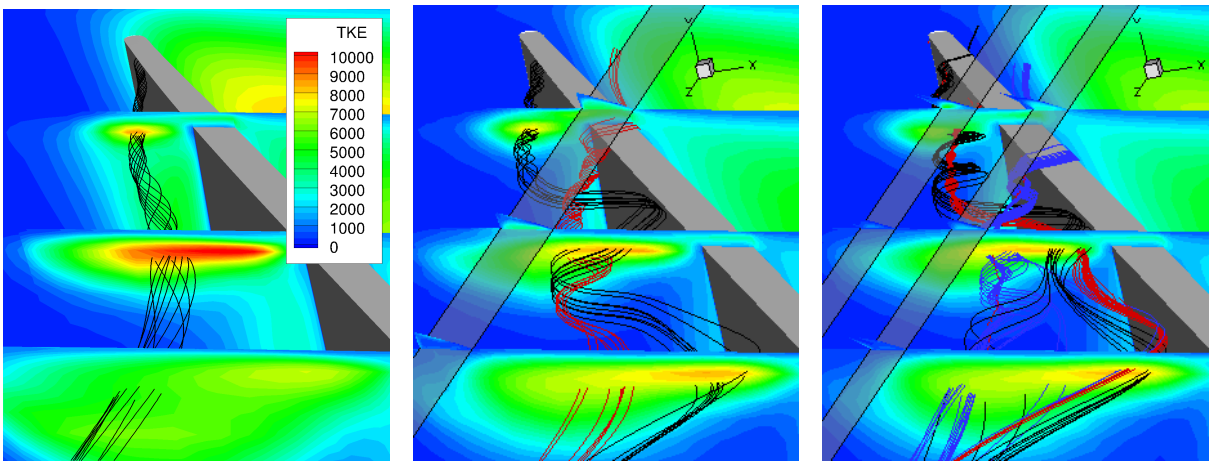

(a) SW Near Surge (b) A1 Near Surge (c) 2*A2 Near Surge

Figure 16: **Turbulent kinetic energy near surge,** $n_{norm} = 90\%$

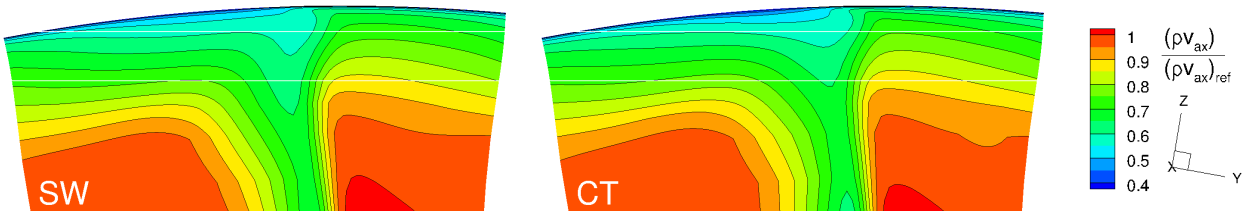

(a) SW Near Surge (b) A1 Near Surge (c)

Figure 17: **Blockage near surge,** $n_{norm} = 90\%$

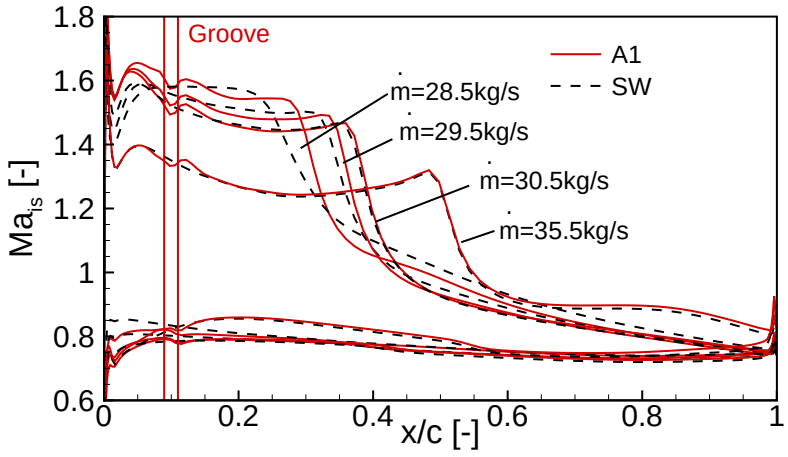

Figure 18: **Isentrop Mach number at 98% blade height.**

types observed are independent and can be combined by using grooves of each type. It is therefore possible to compensate the efficiency losses generated by a groove of type A that is used to increase the surge margin by using a second groove of type B.

The groove type A properties are further analyzed by a parametric study varying certain groove properties of optimized grooves. A further parametric study of grooves of type A shows how important the position and size of the groove are to effectively increase the surge margin. A low downstream angle of the groove has a positive influence on the efficiency, as for design point condition the influence of the groove on the flow should be minimal, which is promoted by a low angle.

Close to surge additional vortices evoked by the grooves influence and interact with the tip leakage vortex resulting in a more stable flow with lower blockage. This leads to an increase in surge margin.

The values of the geometrical parameters of grooves of type A need to lie within narrow margins for the groove to be effective in increasing the surge margin. Therefore it can be assumed that the groove geometry needs to be adjusted carefully for the compressor it is applied to in order to be effective. Future work will analyze how the results obtained can be transferred to other compressors.

ACKNOWLEDGEMENTS

The investigations were conducted as part of the joint research programme COORETEC-turbo in the frame of AG Turbo. The work was supported by the Bundesministerium für Wirtschaft und Technologie (BMWi) as per resolution of the German Federal Parliament under grant number 0327717C. The authors gratefully acknowledges AG Turbo, MAN Diesel & Turbo SE, Rolls-Royce Deutschland Ltd & Co KG and Siemens AG for their support and permission to publish this paper. The responsibility for the content lies solely with its authors.

REFERENCES

[1] Graham Ashcroft, Kathrin Heitkamp, and Edmund Kuegeler. High-order accurate implicit runge-kutta schemes for the simulation of unsteady flow phenomena in turbomachinery. In *Proceedings of the 5th European Conference on Computational Fuild Dynamics ECCOMAS CFD, Lisbon, Portugal*, 2010.

[2] Kai Becker, Kathrin Heitkamp, and Edmund Kuegeler. Recent progress in a hybrid-grid CFD solver for turbomachinery flows. In *Proceedings of the 5th European Conference on Computational Fuild Dynamics ECCOMAS CFD, Lisbon, Portugal*, 2010.

[3] Greg Carnie, Yibin Wang, Ning Qin, and Shahrokh Shahpar. Design optimisation of casing grooves using the zipper layer meshing method. *ASME Conference Proceedings*, 2011(54679):1163–1174, 2011.

[4] Kwang-Jin Choi, Jin-Hyuk Kim, and Kwang-Yong Kim. Design optimization of circumferential casing grooves for a transonic axial compressor to enhance stall margin. *ASME Conference Proceedings*, 2010(44021):687–695, 2010.

[5] Georgios Goinis, Christian Voss, and Eberhard Nicke. Automated optimization of a circumferential groove type casing treatment for a transonic compressor. In *DLRK 2012, Berlin, Germany*, Berlin, 2012.

[6] E M Greitzer, J P Nikkanen, D E Haddad, R S Mazzawy, and J D Joslyn. A fundamental criterion for the application of rotor casing treatment. *Journal of Fluids Engineering*, 101:237–243, 1979.

[7] Michael D. Hathaway. Passive endwall treatments for enhancing stability. Technical Report TM-2007-214409, NASA, 2007.

[8] Tim Houghton and Ivor Day. Enhancing the stability of subsonic compressors using casing grooves. *Journal of Turbomachinery*, (133), 2011.

[9] E. Johann, B. Mück, and J. Nipkau. Experimental and numerical flutter investigation of the 1[sup st] stage rotor in 4-stage high speed compressor. *ASME Conference Proceedings*, 2008(43154):769–778, 2008.

[10] Martin Mueller, Heinz-Peter Schiffer, and Chunill Hah. Effect of circumferential grooves on the aerodynamic performance of an axial single-stage transonic compressor. *ASME Conference Proceedings*, 2007(47950):115–124, 2007.

[11] V. Perrot, A. Touyeras, and G. Lucien. Detailed cfd analysis of a grooved casing treatment on an axial subsonic compressor. In *Proceedings of European Turbomachinery Conference*, 2007.

[12] D. C. Rabe and C. Hah. Application of casing circumferential grooves for improved stall margin in a transonic axial compressor. *ASME Conference Proceedings*, 2002(3610X):1141–1153, 2002.

[13] L. Reid and R. D. Moore. Performance of single-stage axial-flow transonic compressor with rotor and stator aspect ratios of 1.19 and 1.26, respectively, and with design pressure ratio of 1.82, 1978.

[14] R. Schnell, M. Voges, R. Mönig, M. W. Müller, and C. Zscherp. Investigation of blade tip interaction with casing treatment in a transonic compressor - part ii: Numerical results. *Journal of Turbomachinery*, 133(1):011008, 2011.

[15] U. Siller, C. Voss, and E. Nicke. Automated multidisciplinary optimization of a transonic axial compressor. In *Proceedings of the 47th AIAA Aerospace Sciences Meeting Including the New Horizons Forum and Aerospace Exposition*, 2009.

[16] M. Voges, R. Schnell, C. Willert, R. Mönig, M. W. Müller, and C. Zscherp. Investigation of blade tip interaction with casing treatment in a transonic compressor - part i: Particle image velocimetry. *Journal of Turbomachinery*, 133:011007, 2011.

[17] Yanhui Wu, Wuli Chu, Haoguang Zhang, and Qingpeng Li. Parametric investigation of circumferential grooves on compressor rotor performance. *Journal of Fluids Engineering*, 132(12):121103, 2010.